# SUPPORTING INFORMATION

## Control of initiation, rate, and routing of spontaneous capillary-driven flow of liquid droplets through microfluidic channels on SlipChip

*Rebecca R. Pompano, Carol E. Platt, Mikhail A. Karymov, and Rustem F. Ismagilov*

### SUPPORTING MOVIES

**SI Movie 1: Aqueous droplets flowing spontaneously on fast-flow chip (Regime I**). Droplets of 0.1M $Fe(SCN)_3$ flowed through 55 mPa·s silicone oil on a dichlorodimethylsilanzied glass chip, with flow rates ~100 - 400 μm/s. Movie plays 2.5x faster than realtime. Scale bar is 500 μm.

**SI Movie 2: Aqueous droplets flowing spontaneously on slow-flow chip (Regime II).** Droplets of 0.1M Fe(SCN)3 flowed through 55 mPa·s silicone oil on a dichlorodimethylsilanzied glass chip with a gap height of 2.9 μm. Flow rates ranged from ~0.5-6 μm/s. Movie plays 600x faster than realtime. Scale bar is 500 μm.

**SI Movie 3: Droplets of citrated human whole blood flowed spontaneously on a FEP-dip coated chip.** The oil phase was FC40 with 1 mg/mL RfOEG. Flow rates were on the order of 100 μm/s. Movie plays 2.5x faster than realtime. Scale bar is 500 μm.

### MATERIALS AND METHODS

**Chemicals and Materials**. All reagents used in this study were purchased from commercial sources and used without additional purification unless otherwise noted. Fluorocarbon oils FC-40 (a mixture of perfluoro-tri-n-butyamine and perfluoro-di-n-butylmethylamine) and FC-3283 were obtained from 3M (St. Paul, MN). The fluorous surfactant 1H,1H,2H,2H-Perfluoro-1-octanol was obtained from Sigma-Aldrich (St. Louis, MO). RfOEG (triethyleneglycol mono[1*H*,1*H*-perfluorooctyl]ether) was synthesized according to published procedures[1], prepared as a stock solution at 100 mg/mL in FC70, and stored at -20°C until use. Tetradecane, puriss grade, olefine free, was obtained from Aldrich (St. Louis, MO, cat. 87140) and purified by filtration through a column of heat-activated alumina. Silicone oil (polydimethylsiloxane, trimethylsiloxy terminated, DMS-T03 and DMS-T15) was obtained from Gelest (Tullytown, PA).

(Tridecafluoro-1,1,2,2 -tetrahydrooctyl) trichlorosilane (Gelest Inc., Morrisville, PA) was used to silanize and render surfaces fluorophilic. Dichlorodimethylsilane (>99.5%) was purchased from Sigma-Aldrich (St. Louis, MO, cat. 440272) and stored wrapped in parafilm in a 4ºC refrigerator, and was used to silanize and render surfaces oleophilic. Teflon Emulsion solution (FEP TE9568) was purchased from Fuel Cell Earth.

CdSe Quantum Dots in toluene were purchased from Ocean Nanotech (Cat: QCO-540-0010). Unconjugated BODIPY fluorophore was purchased from Invitrogen (Cat: D3922).

Soda−lime glass plates coated with chromium and photoresist were purchased from Telic Company (Valencia, CA). Photomasks were purchased from CAD/Art Services, Inc. (Bandon, OR). 30 gauge Teflon tubing (I.D. 370 μm), used for goniometer measurements, was obtained from Weico Wire & Cable (Edgewood, NY).

**Device fabrication.** Glass devices were fabricated by standard photolithography followed by wet-etching with hydrofluoric acid.[2,3] Devices used to test initiation, routing, and flow rates in regime I each contained a single etch depth in each piece of the device (depths given in main text). The devices used to test flow rates in regime II were etched with a single layer on the bottom piece of the device (~78 μm deep), and two layers on the top piece of the device. The first layer contained the channels (~ 85 μm deep in total, including posts) and the second layer contained supporting microposts (~ 2 – 6 μm in depth). Microposts were fabricated according to previously published procedures.[2,4] The depth of each capillary and channel was measured using a profilometer (Dektak 150, Veeco, CA).

Through holes were drilled in the top plate with a 0.035" drill bit (Diamond ball 4F bit, Harvey Tool #74335-C4) for all designs, before surface modification. The face of the chip was protected with Scotch tape during drilling, and holes were drilled from the back of the chip. After removing the tape, glass debris from drilling was removed by sonicating the chips in a 1:1 mixture of water and ethanol for 30 – 60 min in a warm water bath, after which the chips were rinsed with DI water and dried with nitrogen.

**Surface modification with fluorosilane.** Glass chips were modified to be hydrophobic and fluorophilic by fluorosilanization according to a modification of previously published procedures.[2] Chips were oxidized in a plasma cleaner for 100 seconds and immediately transferred into a desiccator. 50 μL of (Tridecafluoro-1,1,2,2 -tetrahydrooctyl) trichlorosilane was injected into the desiccator and vacuum was then applied to perform gas phase silanization for 3 – 4 hours. The silanized glass plates were incubated in a 110°C oven for 30-60 min and then allowed to cool on the bench. Chips were cleaned by sonication in a bath of FC-3283 with perfluorooctanol (10:1 v/v) for 1 min, rinsed two times with 0.5 mL FC-3283, sprayed with 100% ethanol, and blown dry with nitrogen. Chips were stored in clean Petri dishes at room temperature on the bench. To remove fluorosilane before re-silanization of the chips, chips were oxidized for 10 min in a plasma cleaner.

**Surface modification with dichlorodimethylsilane.** Glass chips were modified to be hydrophobic and oleophilic by silanization according to a modification of previously published procedures.[5] The glass plate was cleaned and oxidized in piranha solution (3:1 sulfuric acid:hydrogen peroxide) for 30 min, then washed copiously with DI water and blown dry. If the chips were not completely wetted by water at this point, they were piranha cleaned again or oxidized for 10 min in a plasma cleaner. After cleaning, dry chips were immediately transferred into a dessicator that was kept dry with a dry nitrogen line at all times. 100 μL of dichlorodimethylsilane was injected into the dessicator and a mild vacuum was then applied (-200 mm Hg) to perform gas phase silanization for 45 – 60 min. The vacuum was promptly released, refilling the chamber with dry nitrogen, and the silanized glass chip was cleaned by spraying extensively with chloroform, acetone, and ethanol, and then dried with nitrogen gas. Silanized chips

were stored at room temperature in a dessicant box (< 15% humidity, maintained with Drierite) and were good for at least one week. For resilanization, chips were cleaned with piranha solution (3:1 sulfuric acid:hydrogen peroxide) and silanized again as described above.

**Surface modification by FEP-dipcoating.** Glass chips were cleaned and oxidized in piranha solution as described above. A dipping solution was prepared by mixing 2 parts Millipore water with 1 part Telfon Emulsion stock solution and mixing thoroughly by pipetting up and down. This solution could be reused for up to 1 week, and was sonicated for 30 – 60 seconds before each use. After cleaning, each dry chip was carefully lowered into the dipping solution at a rate of 11 cm/min, then withdrawn from the solution at a rate of ~ 1.8 cm/min. The chip was lowered and withdrawn using a two-way Harvard syringe pump turned on its side, using settings for a 10 μL Hamilton Gastight syringe, at 18 and 3 μL/min for entry into and withdrawal from the solution, respectively). Once withdrawn from solution, the chip was allowed to dry in the air, until the coating turned opaque. After dipping, chips were brought from room temperature to 250°C on an Isotemp hotplate and held at this temperature for 5 min. Chips were allowed to cool on the bench top, then were stored in clean Petri dishes on the bench. This FEP-dipped surface was rough on the micron scale. For re-dipping, first the FEP layer was removed by boiling the chips for 10 min in a 1 M NaOH solution, then washing extensively with water. Excess FEP debris was dislodged from the channels using a scalpel blade. Chips were then piranha cleaned and dipped again as described above.

**Measurement of liquid-liquid surface tension and contact angle hysteresis.** Contact angle and surface tension measurements of aqueous droplets in oil were made using a Rame-Hart Instrument Co. goniometer (model 500-00 Advanced), with DROPimage Advanced software for image acquisition and analysis. Aqueous solution (usually 0.1 M $Fe(SCN)_3$) was loaded into a 50 mL Hamilton Gastight syringe and passed through 30 gauge Teflon tubing to a metal 27 gauge needle. The tip of the metal needle was sheathed with a 5 mm length of Teflon tubing, to prevent wetting of the needle by the aqueous droplet. The sheathed needle was inserted vertically into a bath of hydrocarbon or silicone oil in a glass chamber, which was built by using quick-set epoxy to glue glass microscope slides together.

For surface tension measurements, a hanging droplet was generated by flowing 3 or 4 μL of aqueous solution out of the syringe at a flow rate of 95 μL/min into an oil bath, using a Harvard syringe pump. For each oil, the surface tension was monitored over time (at least 20 min) to determine stability. The equilibrium surface tension was measured for 5 droplets, and had a standard deviation of ± 2 mN/m or less.

Aqueous droplets were extremely slow to equilibrate in high viscosity silicone oil with 6 μM BODIPY fluorophore and 0.01 mg/mL Span-80, and a modified procedure was used. Surface tension for these droplets was determined by flowing 10 μL of aqueous solution out of the syringe at a flow rate of 50 μL/min, and then allowing the droplet to equilibrate for one hour. At the end of the hour, the droplet was shrunk by 5 μL at a flow rate of 20 μL/min. This concentrated the surfactant at the interface and caused an abrupt decrease in surface tension. The droplet was left to reequilibrate for 20 minutes, during which time the surface tension gradually increased and leveled off. The surface tensions obtained by this method were consistent with surface tensions obtained by allowing a pendant droplet to equilibrate overnight (12-14h) and had a standard deviation of ± 3 mN/m (5 droplets).

For advancing and receding contact angle measurements, the substrate of interest was placed in the hydrocarbon or silicone oil bath at the bottom of the glass chamber. The tip of the sheathed metal needle was positioned ~ 2 mm above the substrate, and a hanging aqueous droplet was generated that almost touched the surface of the substrate. Next, while imaging with the DROPimage software, the droplet was advanced by infusing the aqueous solution at a flow rate of 20 μL/min, and then immediately receded by withdrawing the solution at the same flow rate (see SI Figure 1). This procedure moved the three-phase contact line at a velocity of ~ 30 μm/s (measured by time-lapse imaging). The advancing and receding contact angles were measured for 5 droplets, and had an accuracy of ± 1 degree.

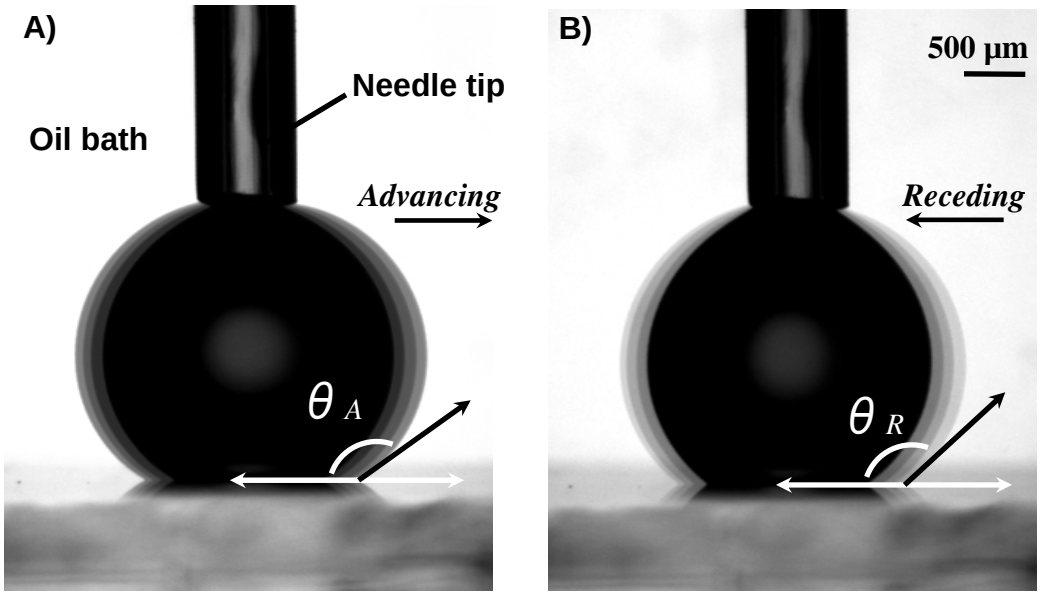


**SI FIGURE 1 –** Overlaid photos taken during contact angle hysteresis measurements on a goniometer. A droplet of 0.1 M $Fe(SCN)_{3,aq}$ solution was advanced and receded under tetradecane on a methylsilanized glass surface, by adding and withdrawing volume through a syringe. Four photos were overlaid for each image, showing the outlines of the droplet during (A) advancing and (B) receding. The contact angles recorded during this experiment were $\theta_A = 148°$ and $\theta_R = 144°$.

**Viscosity measurement.** Viscosity of silicone oils was measured by using calibrated BS/U/M miniature U-tube viscometers manufactured by Cannon Instrument Company (State College, PA). The instructions accompanying the product were followed to take the measurements, and viscosities were measured at room temperature relative to Millipore water. The viscometer was cleaned before use by filling it with chromic acid and letting stand overnight, then rinsing 5 times with Millipore water, then with 100% ethanol, and drying at 65°C for 5 min. The densities used to calculate viscosity were 0.99821 g/mL for water, and 0.898 and 0.960 g/mL for 3 cSt and 50 cSt (nominal) PDMS oils, respectively, according to the product information sheets. The viscosity of the 3 cSt PDMS oil was measured on a M2 viscometer and was 2.76 ± 0.02 mPa·sec (3.08 ± 0.02 cSt). The 50 cSt PDMS oil was measured on M5 viscometer from the same manufacturer and was 55.0 ± 0.1 mPa·sec (57.3 ± 0.1 cSt).

**Slipper.** A homebuilt mechanical slipper was employed to allow for the precise movement of SlipChip plates relative to one another (SI Figure 4, below). The slipper has two movable metal rod assemblies equipped with two adjustable pins each, which fit in four small 1 mm holes drilled in the top plate of the SlipChip. This rod assembly is attached to a 2D high-precision micrometer 460A-XY (Newport Corp., Irvine, CA) with 1 micron sensitivity. The bottom plate is fixed in position using an adjustable edge plate at the back and a spring-loaded lever at the front of the chip; a large gap in the slipper base allows for imaging of the SlipChip. SlipChips can be assembled directly on a slipper just before use.

**General procedure for device assembly and experiments.** Each device consisted of two plates. The bottom plate was fixed into place on the slipper. Approximately 180 μL of oil was pipetted onto the bottom plate, and the top plate was slowly lowered down to be wetted by the oil while avoiding air bubbles, bringing the two plates into close contact. Four holes in the top plate were aligned with the four pins of the slipper to allow controlled slipping. The positions of the pins were adjusted so that the two plates were aligned in the "filling" position.

The device was loaded with aqueous solution by carefully inserting the tip of a 10 μL or 100 μL pipette into the inlet hole and manually loading the solution, then slipping away from the filling position before releasing the pipette. Oil was displaced into the gap between the plates during filling, and an open oil outlet was near, but not connected to, the dead-end of the aqueous channel, to facilitate drainage of oil.[2] After loading, a layer of oil (200 – 800 μL) was added to the top of the chip to ensure that oil flux through the access holes was not limiting. For experiments with specified gap heights, additional steps were taken to control to height of the gap, as described below. Finally, the device was slipped to the "flow" position while imaging the flow of droplets over time.

Images were collected on a Leica MZ16 stereomicroscope with a Spot Insight color camera, model 3.2.0 (Diagnostic Instruments Inc., MI). To determine the flow rate, two images with a known time interval were overlaid, and the distance travelled by the back edge of the droplet in the capillary was measured using the Spot software. Distances were calibrated in the software by collecting an image of a microruler, taken at the same magnification as the images of the device.

**Control of gap height.** Two flat glass plates brought together with oil between them and left unaltered often had a gap between them at least 10 μm in height; the height depended primarily on the rate at which oil could escape during assembly (faster escape leading to a smaller gap), either through exit holes drilled in the top chip or out the edges of the chip. The presence of sparsely-placed physical supports in the gap facilitates escape of oil. We found that physically supporting the gap increased uniformity on a single chip, as well reproducibility between chips. Initially, we suspended silanized glass microspheres[2] in the lubricating oil layer to support the gap, but at the low concentrations required to keep beads out of the etched features, the pressure applied during SlipChip assembly compressed the beads and resulted in a smaller gap than desired. Instead, we used glass microposts etched into the top plate of the SlipChip[2,4]. The height of these posts, plus the distance between the posts and the bottom plate, constituted the gap height. Microposts (100 μm x 100 μm, 900 μm pitch) of both 5-6 and 2-3 μm in height produced a uniform gap with a height that was 1-1.5 μm taller than the height of the posts. As

micropost placement was determined during chip design, posts were precisely positioned to support the gap without inhibiting aqueous flow or oil mobility.

For experiments that required a controlled gap height using etched microposts, we used the following procedure after assembling the chip on the Slipper as described above. The top of the chip was slipped laterally several times to force out excess oil; the chip was then clipped tightly (2 clips, one on each side of the chip, with small magnets applied in the center of the chip) for a minimum of 10 minutes. After this period, the magnets were removed and the tight clips were replaced with 2 looser clips that permitted facile slipping with the slipper while still applying pressure, and the chip was allowed to relax for a period of 15 minutes. The magnets were reapplied, and the chip was filled manually by pipette; after filling, lateral slipping was employed again to force out excess oil. Magnets were removed, the chip was left to relax with loose clips for 20 minutes, and the experiment was continued.

**Measurement of gap height.** Gap heights were measured by loading the SlipChip with fluorescently stained oil, and comparing the fluorescent intensity of channels of known depths to the fluorescent intensity of the gap.[2] The chips were cleaned thoroughly (hexane, acetone, ethanol) after assembly, to remove contaminating fluorescent oil from the chips' surface. We observed that filling with aqueous solution could affect gap height, so the height of the gap was always determined after filling and relaxation as described above.

An accurate measurement required the use of a photostable dye, to avoid rapidly bleaching the gap. Fluorocarbons and tetradecane were stained with CdSe quantum dots by diluting the stock solution (from Ocean Nanotech) 10-fold in the oil of interest. Silicone oils were stained with BODIPY (Invitrogen). BODIPY was prepared as a 3 mM stock solution in chloroform and silicone oil and stored in aliquots at -20 deg C. To prepare a working solution, the stock was diluted 500x into silicone oil for a final concentration of 6 μM BODIPY in the oil. The working solution was vortexed for 2 minutes and sonicated for 30 minutes in a warm water bath before use.

The fluorescent intensity in the gap and in nearby channels was measured on a Leica DMIRE2 inverted fluorescent microscope, using a narrow field diaphragm to exclude emissions from nearby features. The gap was imaged as close to its reference feature as possible to ensure that the gap above the feature was the same as at the adjacent gap. Gap height was calculated according to

$$h_3 = \left( \frac{FI_{gap} h_{feature}}{FI_{feature} - FI_{gap}} \right)$$

where $FI$ is the observed fluorescent intensity [arb. units]; $h_3$ is the height of the gap [μm], and $h_{feature}$ is the height of the feature that was used as a reference [μm]. The gap height was measured at 8 positions on each chip to determine uniformity.

**Calculation of average length of droplet.** Predictions for flow regime II required an estimate of the length of the recirculating oil path, $L_3$. Geometrically, the length of the path of oil flow must be equal to the length of the aqueous droplet. The length of the droplet is time-dependent, decreasing during flow, so an average length, $L_{avg}$, was used. The initial length of the droplet was defined as the length of the

capillary, $L_1$. The final length of the droplet once it has fully entered the channel, $L_{end}$, was calculated from the ratio of the volume of capillary and the cross-sectional area of the channel on the isotropically etched chip:

$$L_{end} = \frac{\left[ w_1 h_1 + h_1^2 (\frac{\pi}{2} - 2) \right] L_1}{w_2 h_2 + h_2^2 (\frac{\pi}{2} - 2)}$$

where $w_1$, $h_1$, $w_2$, and $h_2$ are the maximum width and height of the capillary and the channel, respectively. $L_{avg,}$ was calculated as the average of the initial and final lengths:

$$L_{avg,} = 0.5(L_1 + L_{3end}).$$

The channel and capillary geometries varied in each condition on the chip, so each condition had a unique value of $L_3 = L_{avg}$ (SI Table 7).

**Description of the side path for oil flow in the capillary.** The side path for oil is irregularly shaped (Fig. 7b), set by the curvature of the glass-etched capillary and the droplet inside it. It was not possible to exactly calculate the flow resistance through this geometry, so we made a first-order approximation of the cross-sectional geometry as a rectangle (*blue boxes* in Fig. 7b*ii*). Microphotographs of the capillary showed a space of 20 μm between the edge of the droplet and the edge of the capillary. This value was used as $h_4$, the narrow dimension of the path. The width of the path was defined as 50 μm, to provide a cross-sectional area (20 x 50 $\mu m^2$) that was roughly equivalent to the more irregular geometry.

**Loading complex biological solutions for flow on SlipChip.** Several biological solutions were tested for their ability to flow spontaneously: 1 mg/mL BSA in phosphate buffered saline, AIM-V culture medium (Gibco, used as received), citrated human whole blood (collected into a Citrate BD Vacutainer tube 1 hour before the experiment), and a PCR buffer solution (1x Pfu solution with 1 mg/mL BSA). Resazurin (0.02%) was added to each of these solutions (except blood) to render them easily visible (blue colored) on chip; this addition did not affect their surface tension significantly. For each experiment, the aqueous solution was loaded slowly onto an FEP dip-coated SlipChip, taking care to avoid pushing solution out into the gap where the oil layer could easily rupture and cause sticking. For BSA, blood, and AIM-V medium, loading was achievable using a micropipette, and these solutions flowed spontaneously without sticking when used with 1 mg/mL RfOEG in FC40. However, the PCR buffer solution had extremely low interfacial tension with this oil (estimated < 5 mN/m), and it was not possible to prevent it from leaking into the gap during manual loading with a pipette. As a result, it could not flow spontaneously. On a device with lower resistance to loading (i.e. wider or deeper channels and fewer sharp turns) or a smaller gap, this problem may be reduced; we observed that with this oil and this surface chemistry, PCR reagents were successfully loaded into larger channels and flowed spontaneously (not shown). We emphasize that PCR reagents were reliably loaded previously, without leaking into the gap, with chips that used tetradecane as the oil and dichlorodimethylsilanized surface chemistry. [5-9]

**Prediction that flow of a droplet will continue once it is initiated, as long as the receiving channel is larger than the capillary:**

Requirement for spontaneous flow: $\Delta P_{cap\,1} > \Delta P_{cap\,2}$

$$2\gamma \cos\theta_R \left(\frac{1}{w_1}+\frac{1}{h_1}\right) > 2\gamma \cos\theta_A \left(\frac{1}{w_2}+\frac{1}{h_2}\right)$$

Rearrangement gives: $$\left(\frac{1}{w_1}+\frac{1}{h_1}\right) > \frac{\cos\theta_A}{\cos\theta_R}\left(\frac{1}{w_2}+\frac{1}{h_2}\right).$$

**Additional supporting figures:**

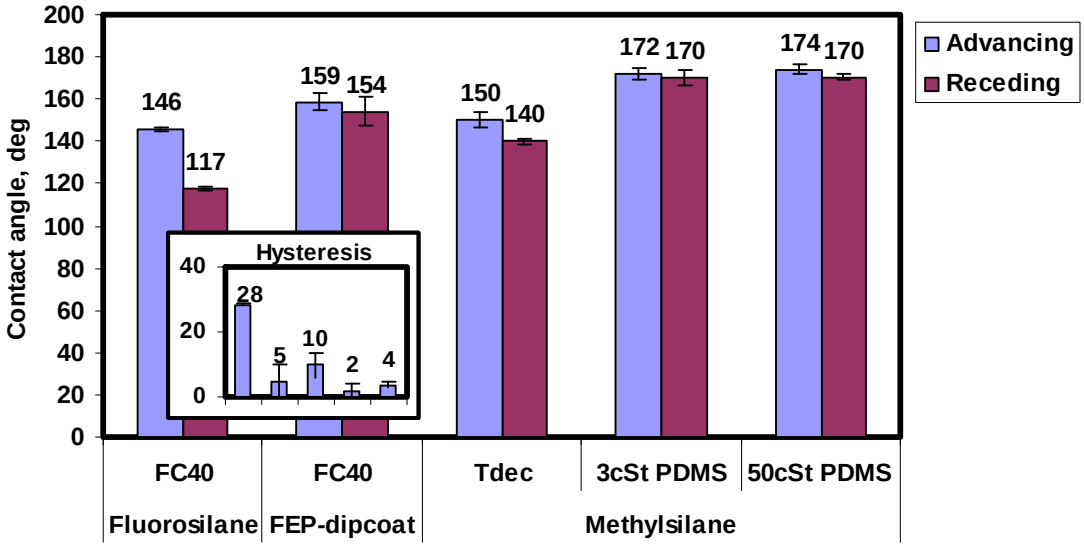


**SI Figure 2.** Advancing and receding contact angle measurements for aqueous droplets of 0.1 M $Fe(SCN)_3$ in oil on glass surfaces modified by protocols described in the text. The inset shows the calculated contact angle hysteresis (advancing – receding angles, in degrees) on each surface. Error bars show 1 standard deviation ($n \geq 5$ droplets)

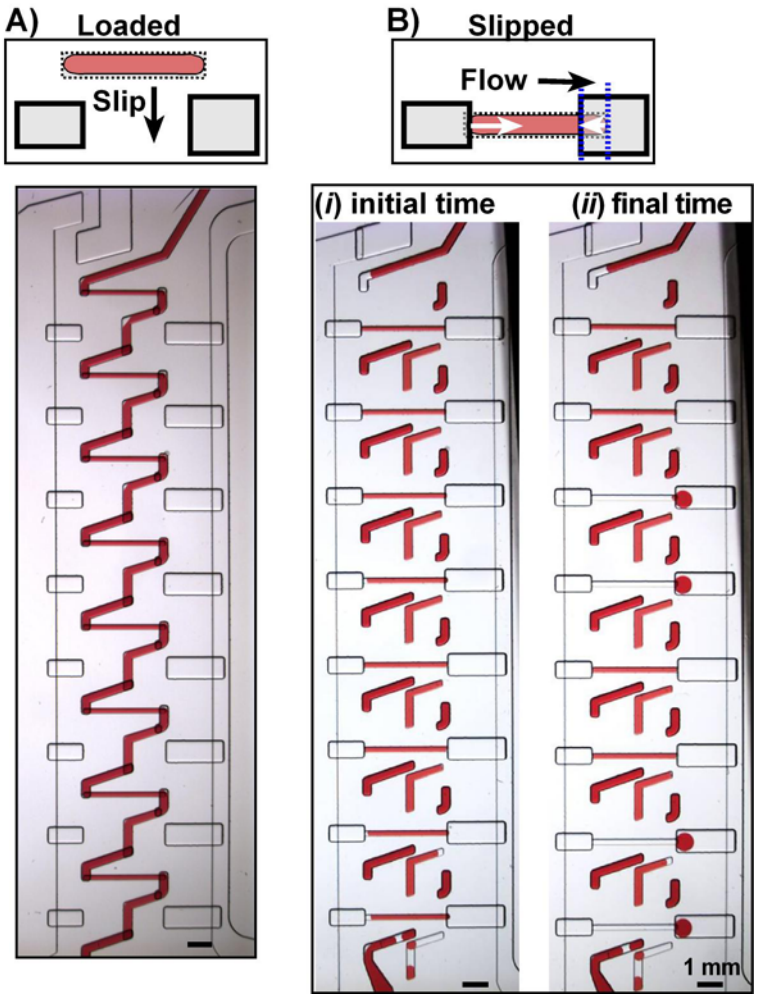


**SI Figure 3.** Schematics and microphotographs of a representative SlipChip used to test initiation of flow, in (A) the filling position and (B) the flow position. The gap between the plates was filled with oil and then an aqueous solution (*red*) was loaded into the chip by pipetting into a drilled inlet hole at the top (not shown in photo). Once the chip was slipped to the flow position (B*i*), droplets could initiate flow or not (B*ii*). In the schematics, dotted lines indicate the bottom plate and bold solid lines indicate the top plate of the SlipChip.

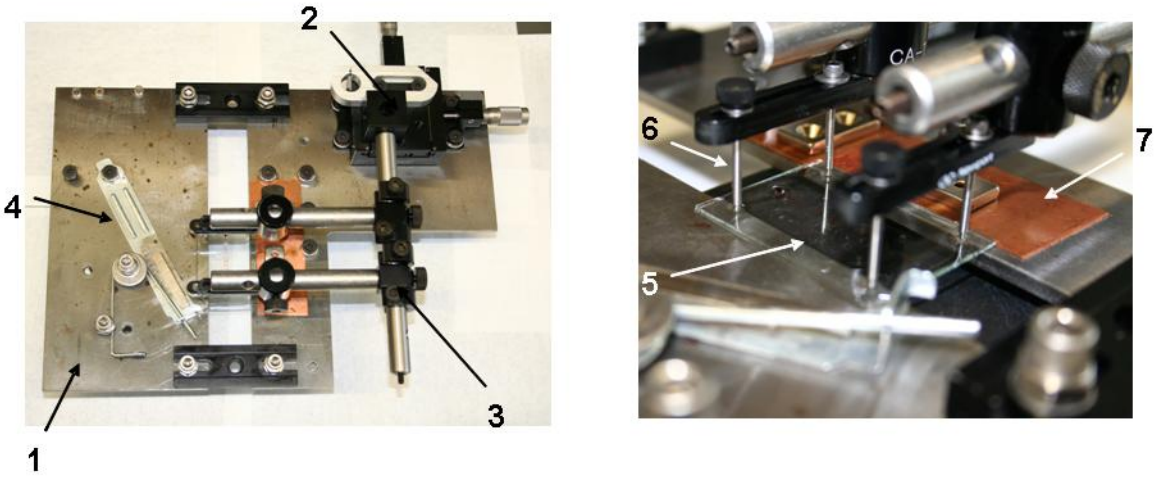


**SI Figure 4.** Image of the assembled mechanical slipper. (left) 1 – base plate of slipper with the imaging gap; 2 – 2D high-precision micrometer; 3 – movable lever assembly; 4 –assembly with spring to fix bottom plate in position; (right) 5 – SlipChip device with four holes in top plate; 6 – adjustable pins; 7 – thin edge metal plate. The SlipChip shown is 1.5 inch x 2 inch in size.

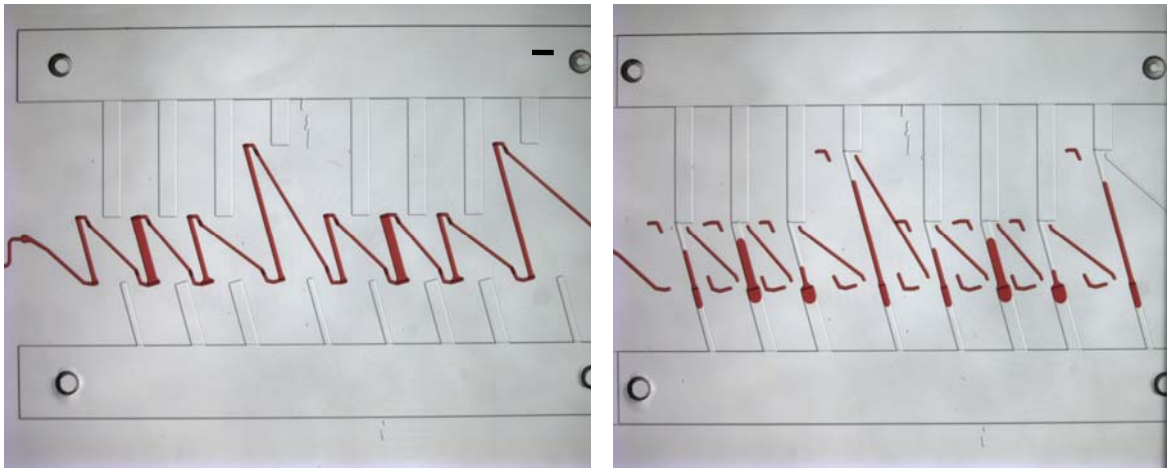

**SI Figure 5.** Microphotographs of a representative SlipChip used to test flow regime I, in *(left)* the filling position and *(right)* the flow position. The gap between the plates was filled with oil and then an aqueous solution (*red*) was loaded into the chip by pipetting into a drilled inlet hole at the right (not shown in photo). Scale bar is 1mm.

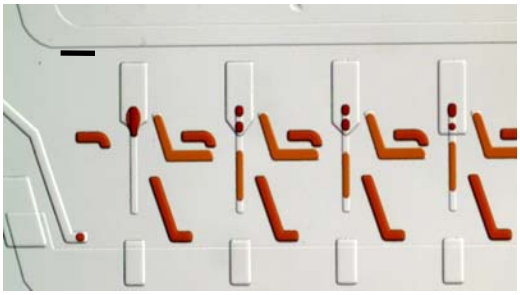

**SI Figure 6.** Microphotograph of an experimental test of different shapes at the junction of the capillary and receiving channel. The surface was treated with dichlorodimethyl silane to provide low contact angle hysteresis; the oil used was tetradecane. The capillary had depth 50 μm, while the channel had depth of 78 μm. The chip was slipped twice, increasing the overlap between the capillary and the channel each time, before the photo was acquired. The three right-hand channel geometries, which had angled and rectangular junctions, each caused the droplet to break after both slips. The left-most channel geometry, a gradual "fluted" expansion in width, minimized break-up of droplets and allowed the entire droplet to flow from the capillary into the channel. Scale bar is 1mm.

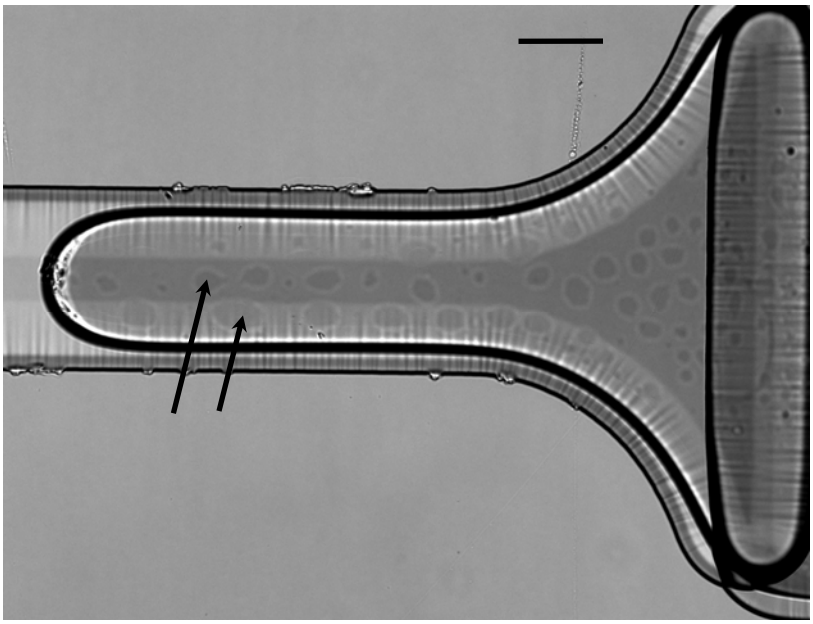

**SI Figure 7.** Microphotograph of a droplet during flow on a SlipChip. Rupture of the oil layer under the aqueous droplet was suggested by the many small regions of oil (*two are marked with arrows*) that were captured underneath the aqueous droplet. The oil in the experiment shown was 55 cSt PDMS oil, loaded onto a chip designed to test Regime II. The aqueous solution was 0.1 M $Fe(SCN)_3$. Scale bar is 100 μm.

**SI Figure 8.** Microphotographs of a representative SlipChip used to test flow regime II, (*left*) after filling, and (*right*) during flow. The gap between the plates was filled with oil and then an aqueous solution (*red*) was loaded into the chip by pipetting into a pair of drilled inlet holes at the bottom (not shown in photo). Droplets flowed from left to right. Scale bar, 1mm.

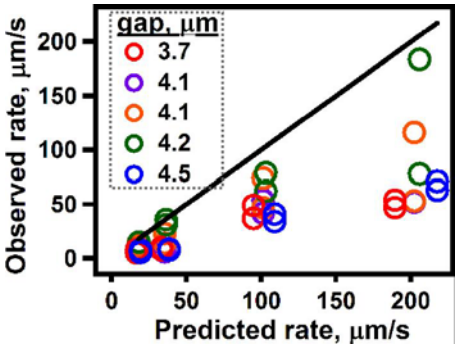


**SI Figure 9.** Plot of observed versus predicted flow rates (µm/s) when oil flowed through the gap and side path, for 3 cSt PDMS oil. Flow rates were measured by tracking the position of the interface between aqueous droplet and the oil in the channel. The height of the gap was measured before each trial (legend) and used to predict the flow rates for that trial using Equation 4 with Equation 8c. All trials were conducted using a chip with 2 µm microposts, with observed gap heights from 3.7 µm to 4.5 µm. Solid line shows prediction.

**Supporting data tables:**

**SI Table 1 – Parameters used for predictions of flow of 0.1 M $Fe(SCN)_3$ aqueous solution in each oil on a dichlorodimethyl-silanized chip.**

| Model parameters | 57 cSt PDMS + Span 80[a] | 57 cSt PDMS + Span 80[a] + BODIPY[b] | 3 cSt PDMS + Span 80[a] | 3 cSt PDMS + Span 80[a] + BODIPY[b] | Tetra-decane | Mineral oil | |
|---|---|---|---|---|---|---|---|
| γ, surface tension | 20 | 24 | 23 | 32 | 54 | 38 | mN/m |
| $\theta_A$, contact angle | 174 | 173 | 169 | 172 | 155 | 155 | Degree |
| $\theta_R$, contact angle | 170 | 169 | 169 | 171 | 145 | 145 | Degree |
| μ-oil, oil viscosity | 55 | 55 | 2.76 | 2.76 | 2.13 | 21 | mPa s |
| μ-aq, aq. viscosity | 1 | 1 | 1 | 1 | 1 | 1 | mPa s |
| Oil density[c] | 0.960 | 0.960 | 0.898 | 0.898 | 0.7629 | 0.850 | $g/cm^3$ |

[a] Span-80 was included at 0.01 mg/mL concentration.

[b] BODIPY was included at 6 μM concentration.

[c] While density was not needed for predictions of flow rate, it was needed for surface tension and viscosity measurements.

**SI Table 2 – Predicted and observed flow rates (μm/s) for fast flow (oil moved through channels), using 55 cSt PDMS oil with 0.01 mg/mL Span 80. Standard errors are for n = 8 measurements for each condition.**

| $L_1$, μm | $w_1$, μm | $w_2$, μm | Cond-ition | **78/68 Obs** | Std Err | **Pred** | **Pred /Obs** | **59/53 Obs** | Std Err | **Pred** | **Pred /Obs** | **39/36 Obs** | Std Err | **Pred** | **Pred /Obs** |
|---|---|---|---|---|---|---|---|---|---|---|---|---|---|---|---|
| 3000 | 200 | 300 | 1 | **248** | 8 | 272 | 1.1 | **160** | 2 | 182 | 1.1 | **50** | 5 | 77 | 1.5 |
| 3000 | 400 | 600 | 2 | **158** | 2 | 142 | 0.9 | **108** | 2 | 103 | 1.0 | **34** | 4 | 38 | 1.1 |
| 3000 | 200 | 600 | 3 | **565** | 11 | 513 | 0.9 | **318** | 6 | 308 | 1.0 | **127** | 13 | 126 | 1.0 |
| 6000 | 200 | 300 | 4 | **220** | 4 | 205 | 0.9 | **136** | 5 | 136 | 1.0 | **46** | 6 | 59 | 1.3 |

**SI Table 3 – Predicted and observed flow rates (μm/s) for fast flow (oil moved through channels), using 3 cSt PDMS oil with 0.01 mg/mL Span 80. Standard errors are for n = 8 measurements for each condition.**

| $L_1$, μm | $w_1$, μm | $w_2$, μm | Cond-ition | **78/68 Obs** | Std Err | **Pred** | **Pred /Obs** | **59/53 Obs** | Std Err | **Pred** | **Pred /Obs** | **39/36 Obs** | Std Err | **Pred** | **Pred /Obs** |
|---|---|---|---|---|---|---|---|---|---|---|---|---|---|---|---|
| 3000 | 200 | 300 | 1 | **3290** | 202 | 5721 | 1.7 | **1745** | 58 | 3519 | 2.0 | **586** | 23 | 1539 | 2.6 |
| 3000 | 400 | 600 | 2 | **2211** | 85 | 3826 | 1.7 | **1096** | 35 | 2126 | 1.9 | **364** | 16 | 828 | 2.3 |
| 3000 | 200 | 600 | 3 | **7804** | 181 | 10870 | 1.4 | **3861** | 145 | 5882 | 1.5 | **1354** | 39 | 2484 | 1.8 |
| 6000 | 200 | 300 | 4 | **2537** | 138 | 4474 | 1.8 | **1610** | 68 | 2493 | 1.5 | **590** | 45 | 1126 | 1.9 |

**SI Table 4 – Predicted and observed flow rates (μm/s) for fast flow (oil moved through channels), using hydrocarbon oils. Channel and capillary depths were 78/68 μm. The number of measurements for each condition, *n*, is given in the table.**

| $L_1$, μm | $w_1$, μm | $w_2$, μm | Cond-ition | **Tetradecane Obs** | Std Err | *n* | **Pred** | **Pred /Obs** | **Mineral oil Obs** | Std Err | *n* | **Pred** | **Pred /Obs** |
|---|---|---|---|---|---|---|---|---|---|---|---|---|---|
| 3000 | 200 | 300 | 1 | **1003** | 474 | 3 | **7122** | 7.1 | **70** | 1 | 2 | **665** | **10** |
| 3000 | 400 | 600 | 2 | **501** | 210 | 3 | **2387** | 4.8 | **41** | 5 | 3 | **210** | **5** |
| 3000 | 200 | 600 | 3 | **2935** | 647 | 4 | **16961** | 5.8 | **217** | 4 | 4 | **1569** | **7** |
| 6000 | 200 | 300 | 4 | **931** | 290 | 4 | **4839** | 5.2 | **54** | 2 | 4 | **475** | **9** |

**SI Table 5 – Predicted and observed flow rates (μm/s) for slow flow (oil moved through gap and sidepath) using 55 cSt PDMS oil. Channels depths were 81.5 μm; 300 μm-wide capillaries were 78 μm deep, 200 μm-wide capillaries were 74 μm deep.**

| $h_3$, μm | $L_1$, μm | $w_1$, μm | $w_2$, μm | Condition | **Obs Left** | **Obs Right** | Pred | Pred/ Obs Left | Pred/ Obs Right |
|---|---|---|---|---|---|---|---|---|---|
| 2.8 | 3000 | 200 | 700 | 1 | **4.1** | **4.2** | 9.3 | 2.2 | 2.2 |
| | 6000 | 200 | 700 | 2 | **2.5** | **2.6** | 4.6 | 1.9 | 1.8 |
| | 3000 | 300 | 500 | 3 | **0.6** | **0.6** | 1.6 | 2.7 | 2.8 |
| | 6000 | 300 | 500 | 4 | **0.5** | **0.4** | 0.8 | 1.7 | 2.1 |
| 2.9 | 3000 | 200 | 700 | 1 | **5.0** | **5.5** | 9.4 | 1.9 | 1.7 |
| | 6000 | 200 | 700 | 2 | **3.5** | **3.3** | 4.7 | 1.3 | 1.4 |
| | 3000 | 300 | 500 | 3 | **0.7** | **1.0** | 1.6 | 2.3 | 1.7 |
| | 6000 | 300 | 500 | 4 | **0.6** | **0.6** | 0.8 | 1.5 | 1.5 |
| 3.5 | 3000 | 200 | 700 | 1 | **5.6** | **7.0** | 10.1 | 1.7 | 1.3 |
| | 6000 | 200 | 700 | 2 | **4.6** | **4.6** | 5.0 | 1.0 | 1.0 |
| | 3000 | 300 | 500 | 3 | **1.5** | **1.6** | 1.8 | 1.1 | 1.0 |
| | 6000 | 300 | 500 | 4 | **1.2** | **0.8** | 0.9 | 0.7 | 1.1 |
| 4.4 | 3000 | 200 | 700 | 1 | **16.6** | **11.8** | 11.7 | 0.7 | 1.0 |
| | 6000 | 200 | 700 | 2 | **8.8** | **6.7** | 5.9 | 0.7 | 0.9 |
| | 3000 | 300 | 500 | 3 | **2.9** | **2.9** | 2.1 | 0.7 | 0.7 |
| | 6000 | 300 | 500 | 4 | **1.7** | **0.9** | 1.0 | 0.6 | 1.1 |
| 5.6 | 3000 | 200 | 700 | 1 | **9.7** | **10.9** | 15.2 | 1.6 | 1.4 |
| | 6000 | 200 | 700 | 2 | **5.6** | **5.6** | 7.6 | 1.4 | 1.4 |
| | 3000 | 300 | 500 | 3 | **1.8** | **1.8** | 2.7 | 1.5 | 1.5 |
| | 6000 | 300 | 500 | 4 | **0.8** | **1.2** | 1.3 | 1.6 | 1.1 |
| 5.8 | 3000 | 200 | 700 | 1 | **12.1** | **10.8** | 15.9 | 1.3 | 1.4 |
| | 6000 | 200 | 700 | 2 | **5.8** | **5.8** | 8.0 | 1.3 | 1.3 |
| | 3000 | 300 | 500 | 3 | **2.4** | **--*** | 2.8 | 1.1 | N/A |
| | 6000 | 300 | 500 | 4 | **2.0** | **2.0** | 1.4 | 0.7 | 0.7 |
| 6.5 | 3000 | 200 | 700 | 1 | **9.0** | **10.6** | 18.9 | 2.1 | 1.8 |
| | 6000 | 200 | 700 | 2 | **4.6** | **5.2** | 9.5 | 2.1 | 1.8 |
| | 3000 | 300 | 500 | 3 | **1.7** | **1.3** | 3.3 | 2.0 | 2.6 |
| | 6000 | 300 | 500 | 4 | **1.8** | **1.3** | 1.7 | 0.9 | 1.3 |
| 6.8 | 3000 | 200 | 700 | 1 | **12.0** | **15.3** | 20.4 | 1.7 | 1.3 |
| | 6000 | 200 | 700 | 2 | **6.9** | **6.6** | 10.2 | 1.5 | 1.6 |
| | 3000 | 300 | 500 | 3 | **2.7** | **1.5** | 3.6 | 1.3 | 2.4 |
| | 6000 | 300 | 500 | 4 | **0.6** | **0.6** | 1.8 | 2.9 | 3.1 |

* The data point was discarded because the droplet was observed to have stopped moving for a period of about two minutes halfway through flow, possibly caught on a defect in the surface.

**SI Table 6 – Predicted and observed flow rates (μm/s) for slow flow (oil moved through gap and sidepath) using 3 cSt PDMS oil. Channels depths were 81.5 μm; 300 μm-wide capillaries were 78 μm deep, 200 μm-wide capillaries were 74 μm deep.**

| $h_3$, μm | $L_1$, μm | $w_1$, μm | $w_2$, μm | Condition | **Obs Left** | **Obs Right** | Pred | Pred/ Obs Left | Pred/ Obs Right |
|---|---|---|---|---|---|---|---|---|---|
| 3.7 | 3000 | 200 | 700 | 1 | **46.6** | **54.0** | 189.4 | 4.1 | 3.5 |
| | 6000 | 200 | 700 | 2 | **48.7** | **36.9** | 94.8 | 1.9 | 2.6 |
| | 3000 | 300 | 500 | 3 | **8.4** | **10.0** | 33.4 | 4.0 | 3.3 |
| | 6000 | 300 | 500 | 4 | **7.6** | **5.3** | 16.7 | 2.2 | 3.2 |
| 4.1a | 3000 | 200 | 700 | 1 | **52.2** | **--*** | 202.2 | 3.9 | N/A |
| | 6000 | 200 | 700 | 2 | **41.9** | **54.3** | 101.2 | 2.4 | 1.9 |
| | 3000 | 300 | 500 | 3 | **6.3** | **13.5** | 35.6 | 5.7 | 2.6 |
| | 6000 | 300 | 500 | 4 | **10.4** | **12.0** | 17.8 | 1.7 | 1.5 |
| 4.1b | 3000 | 200 | 700 | 1 | **53.4** | **115.7** | 202.2 | 3.8 | 1.7 |
| | 6000 | 200 | 700 | 2 | **47.3** | **74.5** | 101.2 | 2.1 | 1.4 |
| | 3000 | 300 | 500 | 3 | **13.7** | **23.4** | 35.6 | 2.6 | 1.5 |
| | 6000 | 300 | 500 | 4 | **12.7** | **10.3** | 17.8 | 1.4 | 1.7 |
| 4.2 | 3000 | 200 | 700 | 1 | **77.9** | **183.8** | 205.8 | 2.6 | 1.1 |
| | 6000 | 200 | 700 | 2 | **61.6** | **78.9** | 103.0 | 1.7 | 1.3 |
| | 3000 | 300 | 500 | 3 | **30.8** | **35.6** | 36.3 | 1.2 | 1.0 |
| | 6000 | 300 | 500 | 4 | **14.8** | **15.2** | 18.2 | 1.2 | 1.2 |
| 4.5 | 3000 | 200 | 700 | 1 | **63.1** | **71.4** | 217.7 | 3.4 | 3.0 |
| | 6000 | 200 | 700 | 2 | **34.3** | **41.3** | 109.0 | 3.2 | 2.6 |
| | 3000 | 300 | 500 | 3 | **8.6** | **7.7** | 38.4 | 4.5 | 5.0 |
| | 6000 | 300 | 500 | 4 | **7.6** | **5.6** | 19.2 | 2.5 | 3.4 |

*The data point was discarded because the droplet moved too quickly to be captured at the frequency of imaging used for this trial.

**SI Table 7 – Calculated values of the average length of the droplet, $L_{avg}$, on chips used to test flow regime II. These values were used to describe the length of the path of oil flow, $L_3$.**

| **Condition** | **$L_1$, μm** | **$w_1$, μm** | **$w_2$, μm** | **$L_{3\,avg}$, μm** |
|---|---|---|---|---|
| 1 | 3000 | 200 | 700 | 1845 |
| 2 | 6000 | 200 | 700 | 3690 |
| 3 | 3000 | 300 | 500 | 2324 |
| 4 | 6000 | 300 | 500 | 4647 |

**REFERENCES**


(1) Kreutz, J. E.; Li, L.; Roach, L. S.; Hatakeyama, T.; Ismagilov, R. F. *J. Am. Chem. Soc.* 2009, *131*, 6042.

(2) Li, L. A.; Karymov, M. A.; Nichols, K. P.; Ismagilov, R. F. *Langmuir* 2010, *26*, 12465.

(3) Du, W. B.; Li, L.; Nichols, K. P.; Ismagilov, R. F. *Lab Chip* 2009, *9*, 2286.

(4) Li, L.; Du, W.; Ismagilov, R. F. *J. Am. Chem. Soc.* 2010, *132*, 112.

(5) Shen, F.; Du, W. B.; Davydova, E. K.; Karymov, M. A.; Pandey, J.; Ismagilov, R. F. *Analytical Chemistry* 2010, *82*, 4606.

(6) Shen, F.; Du, W.; Kreutz, J. E.; Fok, A.; Ismagilov, R. F. *Lab Chip* 2010, *10*, 2666.

(7) Kreutz, J. E.; Munson, T.; Huynh, T.; Shen, F.; Du, W.; Ismagilov, R. F. *Analytical Chemistry* 2011, *83*, 8158.

(8) Shen, F.; Davydova, E. K.; Du, W. B.; Kreutz, J. E.; Piepenburg, O.; Ismagilov, R. F. *Analytical Chemistry* 2011, *83*, 3533.

(9) Shen, F.; Sun, B.; Kreutz, J. E.; Davydova, E. K.; Du, W. B.; Reddy, P. L.; Joseph, L. J.; Ismagilov, R. F. *J. Am. Chem. Soc.* 2011, *133*, 17705.